

# RSC Advances



This is an *Accepted Manuscript*, which has been through the Royal Society of Chemistry peer review process and has been accepted for publication.

*Accepted Manuscripts* are published online shortly after acceptance, before technical editing, formatting and proof reading. Using this free service, authors can make their results available to the community, in citable form, before we publish the edited article. This *Accepted Manuscript* will be replaced by the edited, formatted and paginated article as soon as this is available.

You can find more information about *Accepted Manuscripts* in the [Information for Authors](#).

Please note that technical editing may introduce minor changes to the text and/or graphics, which may alter content. The journal's standard [Terms & Conditions](#) and the [Ethical guidelines](#) still apply. In no event shall the Royal Society of Chemistry be held responsible for any errors or omissions in this *Accepted Manuscript* or any consequences arising from the use of any information it contains.

**Phase stability and elastic properties of  $(W_{0.5}Al_{0.5})C$  phase with novel  
NiAs-type structure**

L. L. Wang, M. Zhao and Q. Jiang\*

*Key Laboratory of Automobile Materials (Jilin University), Ministry of Education,  
and School of Materials Science and Engineering, Jilin University, Changchun  
130022, China*

**Abstract**

Using density-functional theory, we show that the NiAs-type is more favorable structure for  $(W_{0.5}Al_{0.5})C$  phase than the experimentally proposed WC-type structure when we compare the thermodynamic, dynamic and elastic properties of the two types. Furthermore, it is found that this NiAs-type  $(W_{0.5}Al_{0.5})C$  phase could be synthesized under pressures of 12 GPa or higher, while the advanced mechanical properties of  $(W_{0.5}Al_{0.5})C$  phase, including the bulk modulus of  $B = 268$  GPa, the shear modulus of  $G = 206$  GPa, and the hardness of  $H_V = 30$  GPa, could be reproduced by the NiAs-type structure. The fantastic mechanical properties of the phase are attributed to the synergistic effect of stronger C-Al bonding and weaker C-W bonding of NiAs-type structure.

---

\* Corresponding author. Fax: 86-431-85095371; E-mail: [jiangq@jlu.edu.cn](mailto:jiangq@jlu.edu.cn)

## Introduction

The carbides of transition metal in the group IVB, VB, and VIB columns of the periodic table are well known for their great hardness and strength, high melting temperatures and good corrosion resistance. Because of these advanced properties they are widely applied in technological devices and tools, such as cutting tools, drill bits and rocket nozzles, under high temperature and high pressure. A number of experimental and theoretical efforts have been carried out to understand fundamental properties of these technologically important materials.<sup>1</sup> In the viewpoints of structures, it is noteworthy that group IVB (Ti, Zr and Hf) and VB (V, Nb and Ta) carbides have the cubic rock salt structure with a large variation of carbon content while group VIB (Cr, Mo and W) carbides have a hexagonal structure at room temperature. However, except the tungsten monocarbide, others of group VIB carbides are generally less stable and can be formed only by quenching from high temperature.<sup>2,3</sup>

Recently, Ma *et al.* reported that a special class of new carbide ( $W_{1-x}Al_x$ )C with the hexagonal WC structure has been synthesized by mechanical alloying techniques where some  $W^{4+}$  ions are replaced by  $Al^{3+}$  ions.<sup>4-7</sup> Although the commercial price of Al is much cheaper than that of W, this carbide has excellent mechanical properties. In order to understand the mechanical properties, it is suggested that the excess negative charge arising from the replacement can be balanced by the relevant C vacancy based on theoretical and experimental works.<sup>8-10</sup> However, previous theoretical results show that the ( $W_{0.5}Al_{0.5}$ )C phase with 25% C vacancy has the highest shear modulus  $G = 96$

GPa among all considered structures,<sup>10</sup> which is still lower than experimental results.<sup>8</sup> Thus, the high hardness ( $H_V$ ) of  $(W_{0.5}Al_{0.5})C$  phase should be reconsidered theoretically, and other possible atomic structures must be explored.

It is known that only the positions of the metal atoms can be directly determined by x-ray diffraction in transition metal carbides or borides, whereas the arrangements of the light elements included carbon and boron atoms are speculated from space considerations due to the large mass difference between transition metal atoms and carbon or boron atoms.<sup>11-13</sup> Thus, based on x-ray diffraction results, some different structures of  $(W_{0.5}Al_{0.5})C$  phase could be generally suggested. If the new simulated structure could correspond not only to the experimental results of the mechanical properties, but also the x-ray diffraction results, the new structure should be confirmed, which could also initiate designing new alloys with new properties.

In this work, two candidate structural types of  $(W_{0.5}Al_{0.5})C$  phases are chosen, namely, WC-type and NiAs-type. Their thermodynamic and dynamic stabilities, mechanical and electronic properties are determined by using density functional theory (DFT). The results show that the NiAs-type is more favorable than WC-type. Moreover, it is validated that the pressure will thermodynamically stabilize the  $(W_{0.5}Al_{0.5})C$  phase. The energy barrier of structural transition from WC-type to NiAs-type is also calculated by the transition state search method to understand the kinetic stability of  $(W_{0.5}Al_{0.5})C$  phase.

### Simulation details

Calculations have been performed by CASTEP<sup>14</sup> code using DFT<sup>15,16</sup> and

employing exchange-correlation effects within the generalised gradient approximation (PW91)<sup>17</sup> using Vanderbilt's ultrasoft pseudopotential<sup>18</sup>. Geometry optimization was performed using the BFGS method<sup>19</sup> with a plane-wave cutoff energy of 410 eV. Monkhorst-Pack  $k$  point meshes<sup>20</sup> with a grid of approximate  $0.025 \text{ \AA}^{-1}$  for Brillouin zone sampling were chosen to achieve the total energy convergence of less than  $5 \times 10^{-6}$  eV/atom, the maximum Hellmann-Feynman force within  $0.01 \text{ eV/\AA}$ , the maximum ionic displacement within  $5 \times 10^{-4} \text{ \AA}$  and the maximum stress within 0.02 GPa. The elastic constants  $c_{ij}$  were calculated by  $c_{ij} = \sigma_i / \epsilon_j$  where  $\sigma$  and  $\epsilon$  denote elastic stress and strain, respectively, where the subscripts  $i$  and  $j$  show the Cartesian coordinates of the considered structures.<sup>21</sup> The criteria for convergence of optimization on internal atomic freedoms was selected so that the difference in the total energy was within  $1 \times 10^{-6}$  eV/atom, the maximum force was within  $0.002 \text{ eV/\AA}$ , the maximum displacement was within  $1 \times 10^{-4} \text{ \AA}$ , respectively. The bulk modulus  $B$  and  $G$  were estimated via the Voigt-Reuss-Hill (VRH) average scheme.<sup>22</sup>

The atomic configurations of the NiAs-type and WC-type structures used in our investigations are shown in Fig. 1. It is noteworthy that one can obtain different configurations based on actual arrangement of atoms in the metallic sublattice for the  $(\text{W}_{0.5}\text{Al}_{0.5})\text{C}$  phase. For the NiAs-type and WC-type structures, in this work, two extreme situations were considered: one arranges W/Al on the close-packed-like (0001) facet with equal atomic numbers shown in Figs. 1a and 1c, another is that W or Al is completely located on (0001) facet shown in Figs. 1b and 1d, denoted as T1 and T2 configurations, respectively. We carried out geometry optimization to determine

the equilibrium structures of the  $(W_{0.5}Al_{0.5})C$  phase with T1 and T2 configurations in both cases. In order to evaluate the thermodynamic stability of these configurations, we calculated their formation enthalpies by using the following formula:

$$\Delta H_f = [H_{tot} - (0.5H_W + 0.5H_{Al} + H_{graphite}/4)]/2$$

where  $H_{tot}$  represents the calculated total enthalpy of  $(W_{0.5}Al_{0.5})C$  phase with NiAs-type and WC-type at 0 K and at given pressure, and  $H_W$ ,  $H_{Al}$  and  $H_{graphite}$  represent the enthalpy of elemental W with body-center-cubic structure,<sup>23</sup> elemental Al with face-center-cubic structure<sup>24</sup> and pure hexagonal graphite,<sup>25</sup> respectively. The phonon frequencies were determined by the density functional perturbation theory method (DFPT).<sup>26</sup> This method allows us to calculate phonon frequencies at arbitrary wave vectors  $q$  without use of supercells. Currently, norm-conserving pseudopotentials are required for DFPT calculations of phonon properties.<sup>27,28</sup> The use of a plane-wave kinetic energy cutoff of 750 eV and adoption of  $10 \times 10 \times 6$   $k$ -point sampling were shown to give excellent convergence of total energies.

## Results and discussion

For the considered WC-type and NiAs-type configurations of  $(W_{0.5}Al_{0.5})C$  phase, the order of the relative stability is NiAs-T2 > WC-T2 > NiAs-T1 > WC-T1, resulting from the calculated  $\Delta H_f$  values of  $0.147 < 0.266 < 0.282 < 0.459$  eV/atom shown in Table 1. We therefore focus on T2 structures since the structure owns lower  $\Delta H_f$  values as shown in Table 1, namely NiAs-T2 type of trigonal symmetry ( $P-3m1$ ) and WC-T2 type of hexagonal symmetry ( $P-6m2$ ). The  $\Delta H_f$  value of the former is lower than that of the latter, and the total enthalpy difference  $[H_{tot}(\text{NiAs-type}) -$

$H_{\text{tot}}(\text{WC-type})]$  between the two configurations is  $-0.119$  eV/atom. Thus, it is concluded that the  $(\text{W}_{0.5}\text{Al}_{0.5})\text{C}$  phase of NiAs-type exhibits a better thermodynamic stability than that of the WC-type. In order to further confirm its stability, we have also calculated their total enthalpy difference based on other functionals. The corresponding values are  $-0.113$  eV/atom and  $-0.082$  eV/atom by local density approximation (LDA)<sup>29</sup> and the Heyd-Scuseria-Ernzerhof (HSE06) hybrid functionals<sup>30-32</sup>, respectively. The both values are similar to that attained by GGA functional. Moreover, as shown in Table 1, all  $\Delta H_f$  values based on the GGA calculation are positive. Thus, all of these structures are metastable at ambient condition.

Fig. 2a shows the effect of the pressure ( $P$ ) on the phase stability of these phases. It is clear that NiAs-type can be synthesized under  $P > 12$  GPa while WC-type can be done under  $P > 15$  GPa. Both theoretically determined pressures are higher than the experimental sintering pressures ( $\sim 4$  GPa).<sup>6</sup> The discrepancy could mainly be attributed to the known large kinetic energy barrier in the formation of the carbides. Among optimized lattice constants of the  $(\text{W}_{0.5}\text{Al}_{0.5})\text{C}$  phase ( $a = 2.988 \text{ \AA}$ ,  $c = 5.284 \text{ \AA}$  for NiAs-type and  $a = 3.000 \text{ \AA}$ ,  $c = 5.310 \text{ \AA}$  for WC-type), the  $a$  values are in agreement with the experimental value of  $a = 2.909 \text{ \AA}$ , whereas the  $c$  values are generally smaller than the experimental value of  $c = 5.682 \text{ \AA}$ .<sup>8</sup> This difference could partly come from the calculated scheme. Naturally, the smaller  $c$  values should be attributed to the stacked metal layers of  $\text{Al}^{3+}$  with smaller ionic radius ( $r = 0.535 \text{ \AA}$ )<sup>33</sup> and more shallow valence electronic shell ( $3s^2 3p^1$ ) than those of  $\text{W}^{4+}$  ( $0.660 \text{ \AA}$ )<sup>33</sup> and

$5s^2 5p^6 5d^4 6s^2$ ).

The phonon dispersion curves of  $(W_{0.5}Al_{0.5})C$  phase with the NiAs-type and WC-type structures at  $P = 0$  GPa are present in Figs. 2c and 2d, respectively. It is observed that the phonon frequency of a transverse acoustic (TA) mode is imaginary at the  $A$  (0, 0, 0.5) point in the WC-type structure, which implies that the WC-type structure is dynamically unstable. Thus, only NiAs-type structure is dynamically stable according to its positive phonon dispersion in Fig. 2c. However, Ma *et.al* revealed that the  $(W_{0.5}Al_{0.5})C$  phase has a WC-type structure where W site of tungsten monocarbide lattice is substituted by Al.<sup>4-7</sup> Therefore, it is worthwhile to explore the direct correlation between NiAs-type and WC-type structure for  $(W_{0.5}Al_{0.5})C$  phase. As shown in Figs. 1b and 1d, the essential difference between NiAs-type and WC-type structures comes from different carbon stack layers along [0001] direction. In order to evaluate the relative stability of NiAs-type and WC-type structures, we calculated the phase transition energy barriers from WC-type to NiAs-type by the synchronous transit method.<sup>34</sup> As shown in Fig. 2b, this transition energy barrier is 0.790 eV/formula unit, which comes from the movement of C2 atom. According to the Arrhenius equation:

$$k = A_0 \exp [-E_a/(RT)]$$

where  $E_a$  is the activation energy,  $A_0$  is the pre-exponential factor,  $R$  is universal gas constant 8.314 J/(mol·K), and  $T$  is absolute temperature. If  $k/A_0 \approx 10^{-6}$ ,<sup>35</sup> the phase transition occurs thermodynamically at 664 K based on the calculated  $E_a$ . Therefore, the NiAs-type structure is more favorable for  $(W_{0.5}Al_{0.5})C$  phase than WC-type under

the synthesized temperature (1673 – 1873 K).<sup>4-8</sup>

The elastic stability is a necessary condition for a stable crystal. In the classification of six crystal families, the trigonal crystal system is combined with the hexagonal crystal system and grouped into a larger hexagonal family. Consequently, for a stable hexagonal crystal structure,  $c_{ij}$  has to satisfy the elastic stability criteria<sup>36</sup>:  $c_{44} > 0$ ,  $c_{11} - c_{22} > 0$ ,  $[c_{33}(c_{11} + c_{12}) - 2c_{13}^2] > 0$ . As shown in Table 2, these conditions are clearly satisfied for NiAs-type ( $W_{0.5}Al_{0.5}$ )C phase, confirming its mechanical stability, whereas the experimentally proposed WC-type structure is mechanically unstable ( $c_{44} < 0$ ).

Furthermore, we discuss the elastic behavior of NiAs-type structure. Firstly, the  $c_{33} = 673$  GPa represents higher incompressibility along the  $[0\ 0\ 0\ 1]$  direction compared with those along the  $[1\ 0\ \bar{1}\ 0]$  and  $[0\ 1\ \bar{1}\ 0]$  direction ( $c_{11} = c_{22} = 563$  GPa). Moreover, in Table 2, the average bulk modulus  $B$  and shear modulus  $G$  are 268 GPa and 206 GPa for ( $W_{0.5}Al_{0.5}$ )C phase of NiAs-type structure, respectively. Note that  $G = 206$  GPa is the highest within considered structures. It is well known that the  $G$  value of materials quantifies its resistance to the shear deformation, which is a more accurate predictor of hardness than the  $B$  value. Although the  $G = 206$  GPa is little lower than that of tungsten monocarbide ( $G = 280$  GPa) calculated by using the same method, the case is still a hint of high resistance to the shear deformation. We estimate the hardness of NiAs-type structure by using Chen's model<sup>37</sup>:  $H_V = 2(k^2G)^{0.585} - 3$ , which is based on the Pugh modulus ratio  $k = G/B$ .<sup>38</sup> The estimated  $H_V$  of NiAs-type is 30 GPa, which is much higher than the calculated value of 11 GPa for ( $W_{0.5}Al_{0.5}$ )C<sub>0.75</sub>

phase with highest  $G$  value among all WC-type phases.<sup>10</sup> Moreover, the  $H_V$  of 30 GPa is also higher than experimental values (15 GPa<sup>6,8</sup> and  $\sim 22$  GPa<sup>7</sup>). Firstly, the case can be arising from our perfect NiAs-type  $(W_{0.5}Al_{0.5})C$  structure without defects compared with experimental results. Secondly, it can also be arised from the somewhat overestimated  $H_V$  value of Chen's model. For instance, for tungsten monocarbide,  $H_V$  is 29~33 GPa by using this model<sup>37</sup> while the experimental value is 2400 kg/mm<sup>2</sup> (*i.e.* approximate 24 GPa)<sup>39</sup>. Thus, we could conclude that the mechanical behavior of the  $(W_{0.5}Al_{0.5})C$  phase in NiAs-type corresponds to experimental results well.

According to the preceding description, the major difference between WC-type and NiAs-type structures is different carbon stack layers in metal atomic framework along  $[0\ 0\ 0\ 1]$  direction.<sup>2</sup> As a result, Al and W atoms in NiAs-type are octahedrally coordinated by six C atoms, whereas those in the WC-type are trigonal prismaticly coordinated. Correspondingly, there are two the bond angles of  $92^\circ$  and  $88^\circ$  for C-M-C (M = Al, W) of NiAs-type while those of WC-type are always  $87^\circ$ . Thus, it is inevitable that their different coordinated structures would result in the distinct distribution of electron spatially. The maps of charge density difference (crystal density minus superposition of isolated atomic densities) on the  $(0\ 0\ 0\ 1)$  facet for NiAs-type and WC-type are shown in Figs. 3a and 3b, respectively. For the sake of the contrast, the corresponding map of tungsten monocarbide phase is also shown in Fig. 3c. It is obvious that the distributions around C atoms for  $(W_{0.5}Al_{0.5})C$  phase of NiAs-type and WC-type are similar with that of tungsten monocarbide phase along  $[1$

$1 \bar{2} 0]$  direction within the  $(0 0 0 1)$  facet. Thus, it is reasonable that there are similar  $c_{66}$  values between NiAs-type ( $c_{66} = 228$  GPa) and WC-type ( $c_{66} = 217$  GPa), and they are close to  $c_{66} = 235$  GPa of tungsten monocarbide. However, along  $[0 0 0 1]$  direction within  $(1 1 \bar{2} 0)$  facet, the distribution of NiAs-type as shown in Fig. 3d is similar to that of tungsten monocarbide (Fig. 3f) but apparently higher than that of WC-type (Fig. 3e). This difference explains the nature of the negative values of  $c_{44}$  and  $c_{55}$  for WC-type structure due to the weakening of the C-Al and C-W bonding along  $[0 0 0 1]$  direction.

It is essential to get valuable insight into the bonding characteristics of different structures from the corresponding electronic structures. Figs. 4a and 4b show the total and projected density of states (DOS) of NiAs-type and WC-type, respectively, where the position of the Fermi level ( $E_F$ ) as reference energy is defined as zero. The total DOS elucidate that NiAs-type and WC-type have close similarity to a certain extent. Both structures exhibit a finite density of states  $N(E_F)$  at  $E_F$ , showing metallic characteristics. Compared with NiAs-type, the higher  $N(E_F)$  of WC-type means its less stability, consistent with the formation enthalpy calculation results.<sup>40</sup> The characteristics of the stability can also be observed in the total DOS based on LDA and HSE06 functionals shown in Figs. 4c and 4d, respectively. As shown in Fig. 4a, for projected DOS of NiAs-type, when the energy levels are from -2.11 to -0.35 eV below  $E_F$ ,  $Cp-Alp$  bonding is inconsistent with  $Cp-Wd$  bonding, whereas the both bondings are consistent for WC-type shown in Fig. 4b. Namely, although the Al and W atoms of NiAs-type structure have the same atomic occupation sites and C

coordination numbers, they contribute different bondings in  $(W_{0.5}Al_{0.5})C$  phase and exhibit the particularity from Al. Therefore, it is reasonable that the chemical strength of C-Al bonding (bond length  $d = 2.156 \text{ \AA}$ ) for NiAs-type is consistent with that between six coordinated C and Al in  $Al_4C_3$  phase ( $d = 2.167 \text{ \AA}$ ), and stronger than that for WC-type ( $d = 2.190 \text{ \AA}$ ). For NiAs-type, the bonding peaks are located at around -4.00 and -2.91 eV, corresponding to the  $Alp-Wp$  covalent bonding at -4.78 eV. Moreover,  $Cp-Wd$  bonding of NiAs-type arising from -6.62 to -3.39 eV has less overlapping peaks than those of WC-type, which means less covalence and more ionicity of C-W bonding in NiAs-type. These cases are also confirmed by the charge depletion of W and Al atoms of NiAs-type (0.30 e for W and 0.21 e for Al) and WC-type (0.26 e for W and 0.24 e for Al) based on the Hirshfeld charge analysis.<sup>41</sup> As a general view, the NiAs-type structure has stronger C-Al bonding and weaker C-W bonding than the WC-type structure. Thus, we suggest that the synergistic effects of these bondings would result in a high deformation resistance, and the NiAs-type  $(W_{0.5}Al_{0.5})C$  phase should show excellent mechanical behaviors.

## Conclusion

In conclusion, WC-type and NiAs-type structures of  $(W_{0.5}Al_{0.5})C$  phase are proposed. The NiAs-type structure is found to be dynamically and mechanically more favorable than the experimentally proposed WC-type structure. Our calculation suggests that the NiAs-type structure has the lowest formation enthalpy and could be theoretically synthesized under  $P > 12 \text{ GPa}$ . Moreover, the achieved phase has favorable elastic properties of  $B = 268 \text{ GPa}$  and  $G = 206 \text{ GPa}$ . The estimated  $H_V$  value

of 30 GPa confirms its excellent mechanical behavior of  $(W_{0.5}Al_{0.5})C$  phase of NiAs-type, and exhibits its comparability with tungsten monocarbide.

### **Acknowledgments**

We acknowledge the supports from National Key Basic Research and Development Program (Grant No. 2010CB631001).

## References

- 1 L. E. Toth, *Transition Metal Carbides and Nitrides*, Academic Press New York-London, 1971.
- 2 M. Kertesz and R. Hoffmann, *J. Am. Chem. Soc.*, 1984, **106**, 3453-3460.
- 3 D. L. Price and B. R. Cooper, *Phys. Rev. B*, 1989, **39**, 4945-4947.
- 4 H. G. Tang, X. F. Ma, W. Zhao, X. W. Yan and J. M. Yan, *Mater. Res. Bull.*, 2004, **39**, 707-713.
- 5 J. M. Yan, X. F. Ma, W. Zhao, H. G. Tang and C. J. Zhu, *J. Solid State Chem.*, 2004, **177**, 2265-2270.
- 6 J. M. Yan, X. F. Ma, W. Zhao, H. G. Tang, C. J. Zhu and S. G. Cai, *Mater. Res. Bull.*, 2005, **40**, 701-707.
- 7 Z. H. Qiao, X. F. Ma, W. Zhao and H. G. Tang, *Adv. Eng. Mater.*, 2007, **9**, 910-914.
- 8 J. M. Yan, X. F. Ma, W. Zhao, H. G. Tang, C. J. Zhu and S. G. Cai, *Chem. Phys. Chem.*, 2005, **6**, 2099-2103.
- 9 D. V. Suetin, I. R. Shein, V. G. Bamburov and A. L. Ivanovskii, *Dokl. Phys. Chem.*, 2009, **424**, 14-16.
- 10 L. L. Wang, J. S. Lian and Q. Jiang, *J. Appl. Phys.*, 2011, **109**, 073519.
- 11 Y. C. Liang, X. Yuan and W. Q. Zhang, *Phys. Rev. B*, 2011, **83**, 220102.
- 12 Q. Li, D. Zhou, W. T. Zheng, Y. M. Ma and C. F. Chen, *Phys. Rev. Lett.*, 2013, **110**, 136403.
- 13 Y. C. Liang, C. Li, W. L. Guo and W. Q. Zhang, *Phys. Rev. B*, 2009, **79**, 024111.
- 14 S. J. Clark, M. D. Segall, C. J. Pickard, P. J. Hasnip, M. I. J. Probert, K. Refson and a. M. C. Payne, *Z. Kristallogr.*, 2005, **220**, 567-570.
- 15 P. Hohenberg and W. Kohn, *Phys. Rev.*, 1964, **136**, B864-B871.
- 16 W. Kohn and L. J. Sham, *Phys. Rev.*, 1965, **140**, A1133-A1138.
- 17 J. P. Perdew, J. A. Chevary, S. H. Vosko, K. A. Jackson, M. R. Pederson, D. J. Singh and C. Fiolhais, *Phys. Rev. B*, 1992, **46**, 6671-6687.
- 18 D. Vanderbilt, *Phys. Rev. B*, 1990, **41**, 7892-7895.
- 19 B. G. Pfrommer, M. Côté, S. G. Louie and M. L. Cohen, *Journal of Computational*

- Physics*, 1997, **131**, 233-240.
- 20 H. J. Monkhorst and J. D. Pack, *Phys. Rev. B*, 1976, **13**, 5188-5192.
- 21 O. H. Nielsen and R. M. Martin, *Phys. Rev. Lett.*, 1983, **50**, 697-700.
- 22 R. Hill, *P. Phys. Soc.*, 1952, **65**, 349-354.
- 23 R. J. Hemley, H.-k. Mao, G. Shen, J. Badro, P. Gillet, M. Hanfland and D. Häusermann, *Science*, 1997, **276**, 1242-1245.
- 24 Y. Akahama, M. Nishimura, K. Kinoshita, H. Kawamura and Y. Ohishi, *Phys. Rev. Lett.*, 2006, **96**, 045505.
- 25 S. Scandolo, M. Bernasconi, G. L. Chiarotti, P. Focher and E. Tosatti, *Phys. Rev. Lett.*, 1995, **74**, 4015-4018.
- 26 K. Refson, P. R. Tulip and S. J. Clark, *Phys. Rev. B*, 2006, **73**, 155114.
- 27 A. M. Rappe, K. M. Rabe, E. Kaxiras and J. D. Joannopoulos, *Phys. Rev. B*, 1990, **41**, 1227-1230.
- 28 D. R. Hamann, M. Schlüter and C. Chiang, *Phys. Rev. Lett.*, 1979, **43**, 1494-1497.
- 29 D. M. Ceperley and B. J. Alder, *Phys. Rev. Lett.*, 1980, **45**, 566-569.
- 30 J. Heyd, G. E. Scuseria and M. Ernzerhof, *J. Chem. Phys.*, 2003, **118**, 8207-8215.
- 31 J. Heyd, G. E. Scuseria and M. Ernzerhof, *J. Chem. Phys.*, 2006, **124**, 219906.
- 32 A. V. Krukau, O. A. Vydrov, A. F. Izmaylov and G. E. Scuseria, *J. Chem. Phys.*, 2006, **125**, 224106.
- 33 <http://abulafia.mt.ic.ac.uk/shannon/radius.php?Element=Al>,  
<http://abulafia.mt.ic.ac.uk/shannon/radius.php?Element=W>.
- 34 N. Govind, M. Petersen, G. Fitzgerald, D. King-Smith and J. Andzelm, *Computational Materials Science*, 2003, **28**, 250-258.
- 35 F. Huang and J. F. Banfield, *J. Am. Chem. Soc.*, 2005, **127**, 4523-4529.
- 36 J. F. Nye, *Physical properties of crystals: their representation by tensors and matrices*, Oxford University Press, 1985.
- 37 X. Q. Chen, H. Y. Niu, D. Z. Li and Y. Y. Li, *Intermetallics*, 2011, **19**, 1275-1281.
- 38 S. F. Pugh, *Philos. Mag.*, 1954, **45**, 823 - 843.
- 39 J. F. Shackelford and W. Alexander, 2001.
- 40 H. Jones, *Proc. R. Soc. A*, 1934, **147**, 396-417.

41 F. L. Hirshfeld, *Theoret. Chim. Acta*, 1977, **44**, 129-138.

Table 1 Optimized equilibrium lattice parameters  $a$ ,  $b$ , and  $c$  (Å), calculated formation enthalpy per atom  $\Delta H_f$  (eV/atom) at 0K and 0 GPa for  $(W_{0.5}Al_{0.5})C$  phase of NiAs-type and WC-type with T1 and T2 configurations, respectively.

Space group	WC-type		NiAs-type	
	T1	T2	T1	T2
	<i>Pnmm</i>	<i>P-6m2</i>	<i>Imm2</i>	<i>P-3m1</i>
$a=b$	5.939	3.000	6.096	2.988
$c$	5.447	5.310	5.233	5.284
$\Delta H_f$	0.459	0.266	0.282	0.147

Table 2 Calculated single-crystal elastic constants  $c_{ij}$ , the Hill bulk modulus  $B$ , and shear modulus  $G$  (GPa) for  $(W_{0.5}Al_{0.5})C$  phase of NiAs-type and WC-type with T2 configuration, respectively.

	$c_{11}$	$c_{22}$	$c_{33}$	$c_{12}$	$c_{13}$	$c_{23}$	$c_{44}$	$c_{55}$	$c_{66}$	$B$	$G$
NiAs-type	563	563	673	107	102	102	172	172	228	268	206
WC-type	507	507	573	73	142	142	-26	-26	217	254	18

### Figure captions

Fig. 1 The crystal structures for  $(W_{0.5}Al_{0.5})C$  phase of NiAs-type and WC-type after geometry optimization calculations. (a) and (b) represent T1 and T2 configurations of NiAs-type structure, (c) and (d) represent T1 and T2 configurations of WC-type structure, respectively. Herein,  $a$ -,  $b$ - and  $c$ -axis along  $[1\ 0\ \bar{1}\ 0]$ ,  $[0\ 1\ \bar{1}\ 0]$  and  $[0\ 0\ 0\ 1]$  directions, respectively. Dark large and small balls represent W atoms and C atoms, respectively, light small balls represent Al atoms.

Fig. 2 (a) Predicted formation enthalpies for  $(W_{0.5}Al_{0.5})C$  phase of NiAs-type and WC-type with respect to the elemental decomposition into W, Al and graphite at 0 K and various pressures ( $P$ ). (b) The transition energy barriers of  $(W_{0.5}Al_{0.5})C$  phase from WC-type to NiAs-type. The energy of NiAs-type structure is set to 0 eV/formula unit. Calculated phonon dispersion curves for  $(W_{0.5}Al_{0.5})C$  phase of NiAs-type (c) and WC-type (d).

Fig. 3 The maps of charge density difference (crystal density minus superposition of isolated atomic densities) in the  $(0\ 0\ 0\ 1)$  facet for  $(W_{0.5}Al_{0.5})C$  phase of NiAs-type (a) and WC-type (b) compared with that of tungsten monocarbide (c). (d), (e) and (f) in the  $(1\ 1\ \bar{2}\ 0)$  facets for NiAs-type, WC-type and tungsten monocarbide, respectively. We have removed the regions of lowest density for clarity.

Fig. 4 Total and Partial Density of States (DOS) of atoms for  $(W_{0.5}Al_{0.5})C$  phase of NiAs-type (a) and WC-type (b) based on the GGA functional. Total DOS for NiAs-type and WC-type based on LDA (c) and HSE06 (d) functionals, respectively. The Fermi energy  $E_F$  is shown as a vertical dashed line.

Fig.1

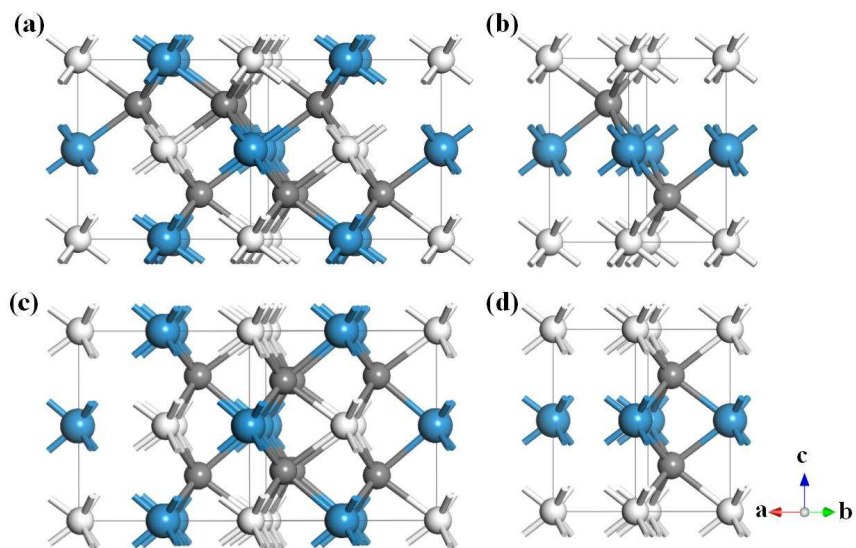


Fig.2

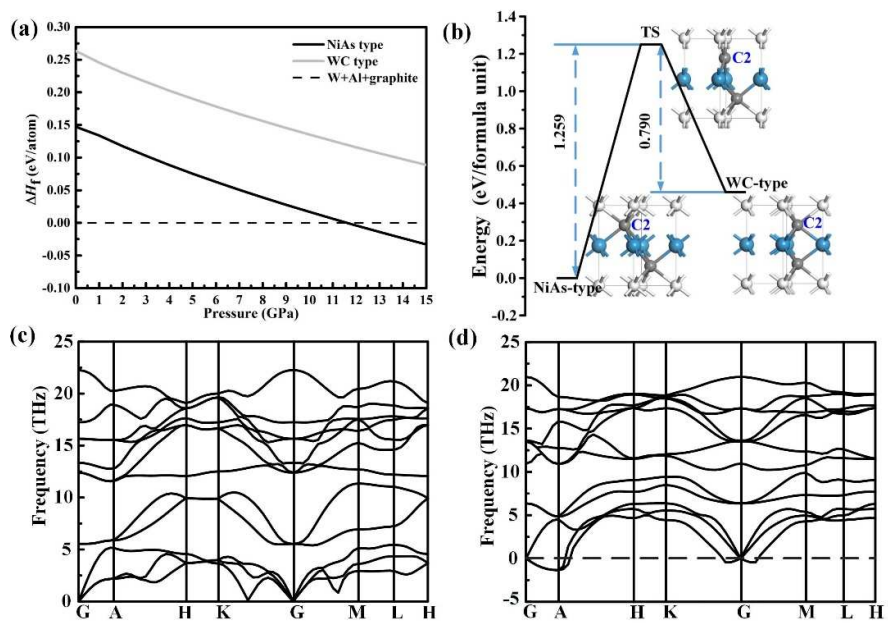


Fig.3

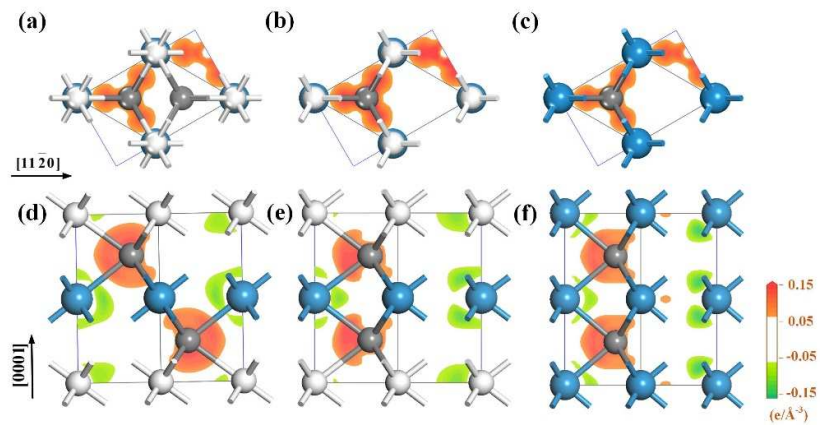


Fig.4

